doi:10.1093/brain/awv048 BRAIN 2015: 138; 1355–1369 | 1355

BRAIN
A JOURNAL OF NEUROLOGY

Memory binding and white matter integrity in familial Alzheimer's disease

Mario A. Parra,[1,2,3,4,5] Heini Saarimäki,[1] Mark E. Bastin,[2] Ana C. Londoño,[5] Lewis Pettit,[1] Francisco Lopera,[5] Sergio Della Sala[1,2] and Sharon Abrahams[1,2,6]

Binding information in short-term and long-term memory are functions sensitive to Alzheimer's disease. They have been found to be affected in patients who meet criteria for familial Alzheimer's disease due to the mutation E280A of the *PSEN1* gene. However, only short-term memory binding has been found to be affected in asymptomatic carriers of this mutation. The neural correlates of this dissociation are poorly understood. The present study used diffusion tensor magnetic resonance imaging to investigate whether the integrity of white matter structures could offer an account. A sample of 19 patients with familial Alzheimer's disease, 18 asymptomatic carriers and 21 non-carrier controls underwent diffusion tensor magnetic resonance imaging, neuropsychological and memory binding assessment. The short-term memory binding task required participants to detect changes across two consecutive screens displaying arrays of shapes, colours, or shape-colour bindings. The long-term memory binding task was a Paired Associates Learning Test. Performance on these tasks were entered into regression models. Relative to controls, patients with familial Alzheimer's disease performed poorly on both memory binding tasks. Asymptomatic carriers differed from controls only in the short-term memory binding task. White matter integrity explained poor memory binding performance only in patients with familial Alzheimer's disease. White matter water diffusion metrics from the frontal lobe accounted for poor performance on both memory binding tasks. Dissociations were found in the genu of corpus callosum which accounted for short-term memory binding impairments and in the hippocampal part of cingulum bundle which accounted for long-term memory binding deficits. The results indicate that white matter structures in the frontal and temporal lobes are vulnerable to the early stages of familial Alzheimer's disease and their damage is associated with impairments in two memory binding functions known to be markers for Alzheimer's disease.

1 Human Cognitive Neuroscience, Psychology, University of Edinburgh, Edinburgh, UK
2 Centre for Cognitive Ageing and Cognitive Epidemiology, University of Edinburgh, Edinburgh, UK
3 UDP-INECO Foundation Core on Neuroscience (UIFCoN), Diego Portales University, Santiago, Chile
4 Alzheimer Scotland Dementia Research Centre and Scottish Dementia Clinical Research Network, NHS Scotland
5 Neuroscience Group, University of Antioquia, Antioquia, Colombia
6 Anne Rowling Regenerative Neurology Clinic, University of Edinburgh, Edinburgh, UK

Correspondence to: Mario A. Parra,
Human Cognitive Neuroscience,
Psychology, University of Edinburgh,
7 George Square,
Edinburgh EH8 9JZ, UK
E-mail: mprodri1@staffmail.ed.ac.uk

Keywords: Alzheimer's disease; memory; structural MR imaging; biomarkers; psychometry

Abbreviations: CC = corpus callosum; CGH = hippocampal part of the cingulum bundle; DT-MRI = diffusion tensor MRI; FWM = frontal white matter; LTM = long term memory; PAL = Paired Associates Learning; STM = short-term memory

Received April 12, 2014. Revised December 29, 2014. Accepted December 30, 2014. Advance Access publication March 11, 2015

Introduction

Although Alzheimer's disease appears to grossly impair integrative memory functions both in short-term memory (STM) (Parra *et al.*, 2009, 2011; Della Sala *et al.*, 2012) and in long-term memory (LTM) (Buschke *et al.*, 1999; Swainson *et al.*, 2001; O'Connell *et al.*, 2004), these impairments seem to have different origins. STM binding supports the temporary retention of conjunctions of features within object representations, a function needed for the formation of new identity. Associative learning (i.e. LTM binding) enables a flexible representation of the relations between the stimulus' parts, each holding its own identity and retaining its individual access (Moses and Ryan, 2006; Mayes *et al.*, 2007).

STM binding deficits have been observed in asymptomatic carriers of the mutation E280A of the *PSEN1* gene (E280A-PSEN1) who still perform normally on LTM binding tasks, such as the Paired Associates Learning (PAL) test of Wechsler Memory Scale (Wechsler, 1997), which has been found to be sensitive to prodromal and clinical Alzheimer's disease (Duchek *et al.*, 1991; Elias *et al.*, 2000). In fact, STM and LTM binding deficits in these individuals do not correlate (Parra *et al.*, 2011) reinforcing the notion of different neural substrates. Whereas LTM binding relies on the integrity of cerebral grey matter structures such as the hippocampus, which is known to be targeted by Alzheimer's disease in its sporadic (Echavarri *et al.*, 2010) and familial variants (Quiroz *et al.*, 2010), a recent functional MRI study indicates that the STM binding function investigated below does not (Parra *et al.*, 2014). Recent behavioural studies have further expanded the evidence in favour of dissociations between these two types of memory representation (Parra *et al.*, 2013).

The STM binding task asks participants to hold together in memory features processed in separate brain regions whereas the LTM binding task (i.e. PAL) asks participants to learn the association between two words. These tasks require effective brain connectivity (O'Reilly *et al.*, 2003; Koenig *et al.*, 2005). It is well recognized that Alzheimer's disease leads to a disconnection syndrome (Bozzali *et al.*, 2011; Gili *et al.*, 2011), and it is therefore hypothesized that such a syndrome underlies this specific cognitive deficit.

An Alzheimer's disease disconnection syndrome has been well characterized using EEG-based methods (Dunkin *et al.*, 1994; Cook and Leuchter, 1996) and more recently by resting state functional MRI (Buckner *et al.*, 2005, 2008). Abnormal patterns of brain connectivity in the default mode network appear to characterize the transition from normal ageing to mild cognitive impairment, and from mild cognitive impairment to Alzheimer's disease (Pihlajamaki and Sperling, 2009; Miao *et al.*, 2011). Furthermore connectivity deficits as assessed by electrophysiological and neuroimaging techniques significantly correlate with cognitive decline both in prodromal (Chua *et al.*, 2008) and clinical Alzheimer's disease (Duan *et al.*, 2006; Medina and Gaviria, 2008). However, the precise contribution of grey and white matter disruptions to the disconnection syndrome, and its cognitive implications, remains unclear (Johnson *et al.*, 2010; Oishi *et al.*, 2011*a*).

Abnormalities in white matter integrity can now be more precisely investigated *in vivo* using diffusion tensor MRI (DT-MRI; Basser, 1995), and have been used to investigate the underpinnings of cognitive deterioration in individuals at increased risk for Alzheimer's disease such as those with mild cognitive impairment (Chua *et al.*, 2008; Stebbins and Murphy, 2009; Bozzali *et al.*, 2011). These studies are characterized by a great variability in the localization of abnormalities within white matter tracts in mild cognitive impairment patients, e.g. in medial temporal lobe (Fellgiebel *et al.*, 2004; Kantarci *et al.*, 2005), projection fibres including posterior cingulum, thalamic radiations and fornix (Kiuchi *et al.*, 2009; Zhuang *et al.*, 2010), association fibres including superior and inferior longitudinal fasciculi and inferior fronto-occipital fasciculus (Medina *et al.*, 2006; Zhuang *et al.*, 2010), and white matter underlying frontal, temporal, parietal and occipital lobes (Medina *et al.*, 2006; Zhuang *et al.*, 2010; Douaud *et al.*, 2011). Nevertheless, recent evidence suggests that these abnormalities are related to cognitive decline in patients with mild cognitive impairment and seem to develop very early along with still subtle grey matter damage (Bozzali *et al.*, 2011; Gili *et al.*, 2011; Sexton *et al.*, 2011).

Studies of preclinical cases of familial Alzheimer's disease have also revealed decreased white matter integrity in columns of the fornix and left orbitofrontal lobe in mutation carriers who have gone on to develop familial Alzheimer's disease, i.e. PSEN1, mutations A431E, L235V, G206A and V717I (Ringman *et al.*, 2007). These patients were completely asymptomatic (Clinical Dementia Rating = 0, cognitively unimpaired) at the time of assessment indicating that reduced white matter integrity may precede the development of clinical symptoms (Ukmar *et al.*, 2008; Wang *et al.*, 2012). Similar disruptions are also observed in other non-Alzheimer's disease dementias (Borroni *et al.*, 2007; Sweed *et al.*, 2012), suggesting that DT-MRI alone may lack specificity in early identification of Alzheimer's disease. However, identifying early DT-MRI abnormalities associated with memory binding impairments, which are known to be sensitive to Alzheimer's disease, would help overcome this limitation. If this hypothesis proves valid, combining assessment of DT-MRI and memory binding performance may unveil brain abnormalities that are more closely related to Alzheimer's disease pathology. The present study therefore firstly investigated whether differences in white matter integrity detected with DT-MRI are related to STM binding deficits in carriers of the mutation E280A-PSEN1 who were either asymptomatic or had recently met criteria for Alzheimer's disease. Secondly the study compared regional DT-MRI metrics with performance on both STM binding and LTM binding tasks

to investigate further the neural dissociation between these two processes.

Materials and methods

Participants

The participants were members of a large kindred from the Colombian province of Antioquia, South America. They carry the gene mutation E280A of *PSEN1*, which invariably leads to an autosomal dominant early-onset familial Alzheimer's disease. This variant of familial Alzheimer's disease becomes clinically detectable at 47 years of age, on average (Lopera *et al.*, 1997) for a clinical description. Mutation carriers either in the symptomatic or presymptomatic stages of the disease, along with members their family, regularly attend clinical and research appointments at the Health Unit of the Neuroscience Centre of the University of Antioquia. This Health Unit has been monitoring this population for more than 20 years. The participants were approached by the responsible consultants who introduced the study and invited them to take part. All the patients who attended the Unit during the time of the study were given the opportunity to participate. Moreover, patients and relatives who had previously expressed an interest in research and whose contact details were held in the centre's database were also contacted. Only those expressing an interest were taken forward to the enrolment process which began with the informed consent. The genetic status of these patients is unknown to the centre's staff and was not revealed to members of the research team until the recruitment process had been completed. This was done using anonymous codes. The study protocol was approved by the Ethics Committee at University of Antioquia, Colombia.

The assessment protocol for all the participants consisted of three phases. First, participants who were not in the centre database (new to the Centre) underwent genetic screening to confirm or exclude the presence of the mutation using the methodology reported by the Alzheimer's disease Collaborative Group (Clark *et al.*, 1995). Second, all the participants underwent neurological and neuropsychological assessments carried out by expert clinicians and neuropsychologists. Third, all the participants underwent DT-MRI assessment. The first two phases allowed us to allocate participants to three groups: (i) participants with familial Alzheimer's disease caused by the E280A single PSEN1 mutation; (ii) carriers of the mutation who did not meet Alzheimer's disease criteria and who were asymptomatic at the time of testing; and (iii) healthy individuals who did not carry the gene mutation, were healthy as confirmed by the clinical interview and were relatives of the members of the other two groups (healthy controls).

A sample of 58 participants entered the study. Data from 32 participants (healthy controls = 6, asymptomatic carriers = 16, familial Alzheimer's disease = 10) were drawn from previous studies investigating visual STM binding (Parra *et al.*, 2010, 2011). The other new participants were assessed with the same protocol. The first group comprised 19 patients with familial Alzheimer's disease diagnosed according to the criteria established by the Diagnostic and Statistical Manual of Mental Disorders (fourth edition, text revision), and the National Institute of Neurological and Communicative Disorders and Stroke and the Alzheimer's Disease and Related Disorders Association (NINCDS-ADRDA) group (McKhann *et al.*, 1984). Second, the asymptomatic carriers group consisted of 18 participants who met neither Alzheimer's disease nor mild cognitive impairment criteria at the time of the testing but who were positive for the E280A mutation. Third, the healthy controls group included 21 non-carriers who were relatives of the patients with familial Alzheimer's disease and asymptomatic carriers. Additional inclusion criteria for the control participants included (i) negative history of neurological or psychiatric disorders; (ii) a Mini-Mental State Examination (MMSE) score $\geqslant 24$; and (iii) no memory complaints as documented by a self-report and family questionnaire.

Asymptomatic carriers and healthy controls were matched according to age, the number of years spent in formal education, and the MMSE scores (Table 1). On average, patients with familial Alzheimer's disease were older and less educated than the two other groups.

Each participant underwent a colour vision assessment using Dvorine pseudo-isochromatic plates (Dvorine, 1963) and a binding perception condition. These assessments were undertaken to rule out the possibility that poor performance on the STM binding task could result from visual or perceptual difficulties. None of the participants recruited for the present study were excluded due to colour vision or perceptual binding problems.

Behavioural assessment

Neuropsychological battery

The neuropsychological battery comprised Spanish translations of the MMSE (Ardila *et al.*, 2000), the PAL Task (Wechsler, 1997), Verbal (Letter-FAS, adapted from Sumerall *et al.*, 1997) and Animal Fluency Tests (from Morris *et al.*, 1989), the Copy and Recall of the Complex Figure of Rey-Osterrieth (Osterrieth, 1944), Part A of the Trail Making Test (Reitan, 1958), the Boston Naming Test (Kaplan *et al.*, 1983), the

Table 1 Demographic variables and cognitive screening

	FAD ($n = 19$)	AC ($n = 18$)	HC ($n = 21$)	ANOVA	*Post-hoc t*-tests (P)		
	Mean (SD), (range)	Mean (SD), (range)	Mean (SD), (range)	F (P-value)	FAD versus HC	AC versus HC	FAD versus AC
Age	47.5 (6.4), (38–66)	35.1 (5.5), (24–43)	39.3 (83), (25–54)	**15.46 (<0.001)**	**0.001**	0.137	**<0.001**
Education	7.3 (3.7), (2–14)	10.2 (3.9), (2–16)	10.3 (27), (4–13)	**4.50 (<0.005)**	**0.024**	0.993	**0.038**
MMSE	23.6 (4.3), (17–30)	29.8 (0.4), (29–30)	29.6 (07), (28–30)	**39.41 (<0.001)**	**<0.001**	0.957	**<0.001**

AC = asymptomatic carriers; FAD = familial Alzheimer's disease; HC = healthy controls; MMSE = Mini-Mental State Examination. Significant ($P < 0.05$) tests highlighted in bold.

Wisconsin Card Sorting Test (Berg, 1948), and the Word List Test (Morris *et al.*, 1989).

Visual short-term memory task

The visual STM task assessed memory for shapes (Fig. 1A), colours, or combinations of the two. Stimuli were randomly selected from a set of eight shapes and eight colours and presented as individual features or as features combined into integrated objects. Each type of stimulus was presented in a separate condition. Three experimental conditions were used (Fig. 1B), each consisting of 15 practice trials followed by 32 test trials leading to a total of 96 test trials per task. Trials were fully randomized across participants and conditions were delivered in a counterbalanced order. In the 'shape only' and 'colour only' conditions, arrays of shapes or colours were presented in the study display. In the test display for the 'different' trials, two new shapes or colours from the study array were replaced with two new shapes or colours. Hence, in these conditions, only visual STM for individual features was required to detect a change. In the 'shape-colour binding' condition, combinations of shapes and colours were presented in the study display. In the test display for 'different' trials, two shapes swapped the colours in which they had been shown in the study display. Hence, memory for bindings of shape and colour in the study display was required to detect this change. No shape or colour was repeated within a given array. Fifty per cent of the test trials were 'same' trials (the study and test displays presented identical items) and 50% were 'different' trials.

Trials began with a fixation screen presented for 500 ms. This was followed by an array presented for 2000 ms on a

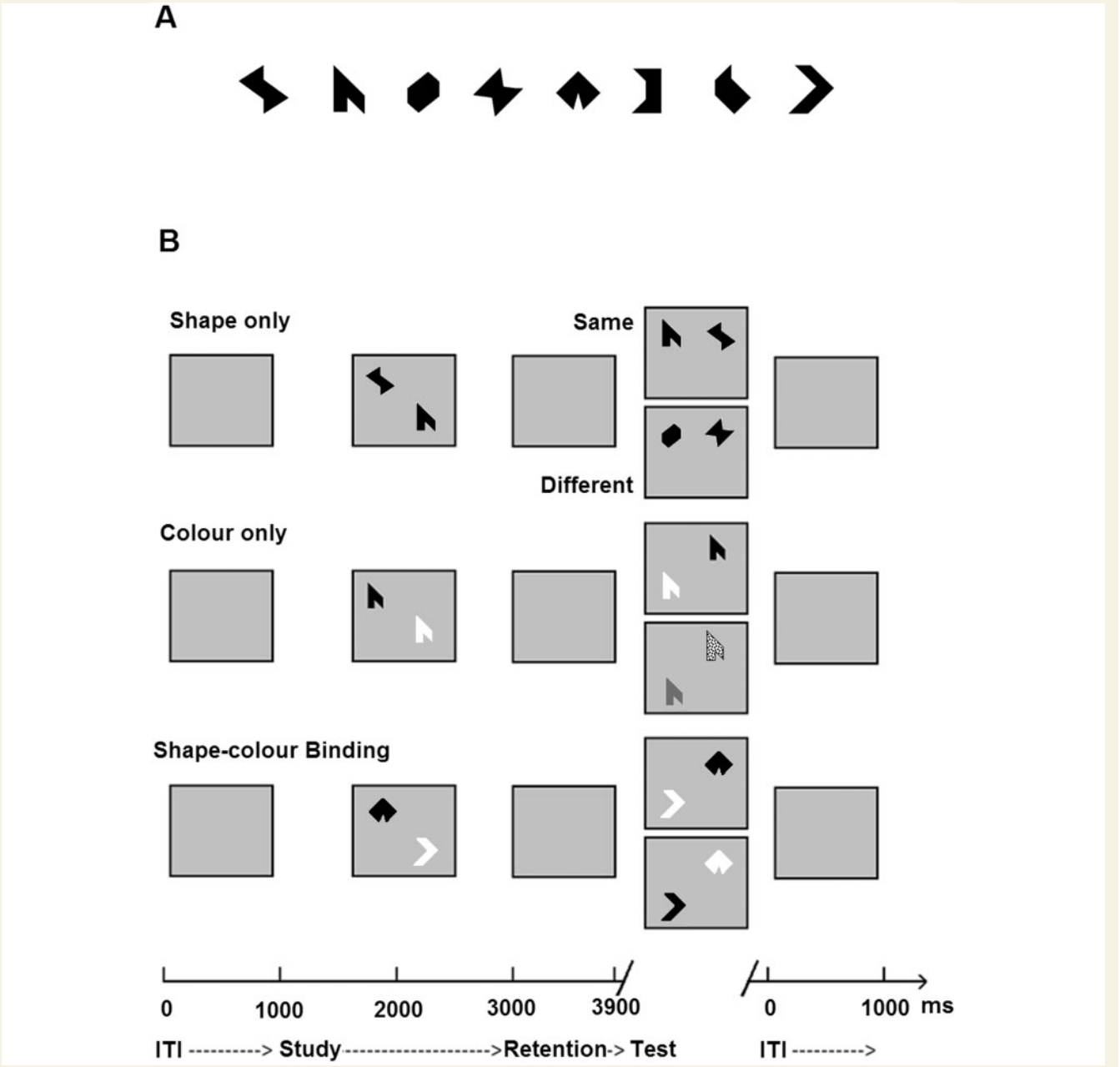

15" PC screen using a 3 × 3 virtual grid ('study display'). After a 900 ms retention interval, participants were presented with 'test display' and were required to respond orally whether the test stimulus was the 'same' or 'different' to the one presented in the 'study display'. The experimenter entered participants' responses using the keyboard.

Memory load was manipulated to match the general group performance by presenting asymptomatic carriers and healthy controls with arrays of three items and patients with familial Alzheimer's disease with arrays of two items. Previous studies have shown that manipulating the memory loads allows performance levels in the baseline memory condition to be equated across groups and, thus, any differences between groups in visual STM binding performance cannot be attributed to the baseline differences in memory for single features (Parra *et al.*, 2010).

DT-MRI assessment

Data collection and preprocessing

DT-MRI data were collected using a Siemens Symphony Vision 1.5 T (Siemens Healthcare Sector) clinical scanner, and consisted of one T_2-weighted and sets of diffusion-weighted (b = 1000 s/mm^2) single-shot, spin-echo, echo-planar volumes acquired with diffusion gradients applied in 12 non-collinear directions. Fifty contiguous slice locations were imaged with a field of view of 220 × 220 mm, an acquisition matrix of 128 × 128 and a slice thickness of 3 mm, giving an acquisition voxel dimension of 1.72 × 1.72 × 3 mm. The repetition and echo times for each echo-planar volume were 7.2 s and 90 ms, respectively.

The DICOM format (http://medical.nema.org) magnitude images were converted into NIfTI-1 format (http://nifti.nimh.nih.gov). Using tools freely available in FSL (FMRIB, Oxford, UK; http://www.fmrib.ox.ac.uk), the DT-MRI data were preprocessed to extract the brain, and bulk patient motion and eddy current induced artefacts removed by registering the diffusion-weighted to the T_2-weighted echo-planar volume for each subject (Jenkinson and Smith, 2001). From these MRI data, mean diffusivity and fractional anisotropy volumes were generated for every subject using DTIFIT.

Region of interest placement

Semi-automated region of interest analysis was performed using 'in house' software written in MATLAB (The MathWorks) that allowed multiple small square regions of interest to be placed on the T_2-weighted echo-planar volumes and then overlaid on the co-registered mean diffusivity and fractional anisotropy maps automatically using locations defined in Montreal Neurological Institute (MNI; http://www.bic.mni.mcgill.ca) standard space. The software allows the user to interactively move regions of interest if standard to native space registration errors cause white matter regions of interest to be placed over CSF or grey matter structures.

The procedure for obtaining the fractional anisotropy and mean diffusivity values for each region of interest is presented in Fig. 2A. First, MNI coordinates were defined in standard space for each region of interest using the ICBM-DTI-81 white matter atlas (Oishi *et al.*, 2011*b*) and then selected in FSLview 3.1.8. Either 4, 6 or 12 square regions of interest were defined for each brain structure depending on its size in horizontal view, sizes of which were 3 × 3 × 1 voxels (see Supplementary Table 1 for MNI coordinates of each region of interest and Supplementary Table 2 for parameters used to place regions of interest). Differences in size of the chosen region of interest are explained by anatomical factors (e.g. tract dimension as for the corticospinal tract) and underlying theory (e.g. middle frontal white matter which encompasses tracts found to be impaired in Alzheimer's disease). An aim of this study was to unveil biomarkers of cognitive impairment in preclinical Alzheimer's disease. We therefore maximized the likelihood of identifying DTI correlates of behavioural impairments.

Several square regions of interest were used for each structure to reduce the effects of differences in individual placement.

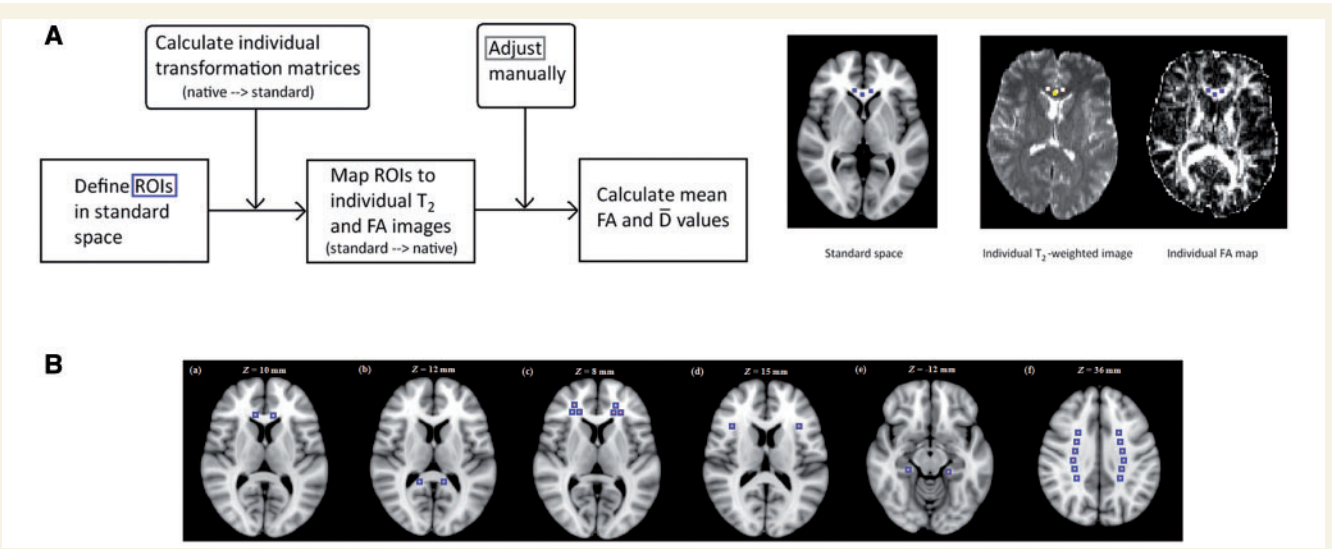

Figure 2 Procedures for DT-MRI assessment. (**A**) Procedures for obtaining fractional anisotropy (FA) and mean diffusivity values for each region of interest (ROI). (**B**) Regions of interest (ROIs) meeting the criteria set for our study: (a) genu CC, (b) splenium CC, (c) middle FWM, (d) inferior FWM, (e) CGH, and (f) centrum semiovale. See 'Materials and methods' section for a detailed description.

Next, the coordinates were mapped from standard space to each individual's T_2-weighted echo-planar volume using the inverse of the transformation matrix from native to standard space (MNI152_T1_1mm_brain template) determined using affine registration (12 degrees of freedom) provided by FSL's FLIRT. The placement of the regions of interest in native space was then checked to ensure no overlap with either CSF or grey matter. The T_2-weighted echo-planar volumes were used to define the regions of interest to avoid biasing their placement by the underlying fractional anisotropy and mean diffusivity values (Bozzali and Cherubini, 2007). Minor adjustments to region of interest position were performed by an investigator blind to subjects' genetic or clinical status. It was only to some regions of interest whenever they fell into CSF or grey matter. Finally, the values for fractional anisotropy and mean diffusivity were obtained for each square and then averaged for each region of interest separately.

We chose regions of interest that met two criteria. First, they comprise tracts relevant to the specific memory functions investigated in this study and second, they have been found to be affected in the preclinical and in the clinical stages of Alzheimer's disease. The regions of interest targeted by the Alzheimer's disease pathology (e.g. amyloid plaques) in the preclinical stages were of particular interest (Buckner *et al.*, 2005; Fleisher *et al.*, 2012). The selected regions of interest that met these criteria are shown in Fig. 2B (see also Supplementary Table 1 for the MNI coordinates). They included two regions of the corpus callosum (CC), the genu (central body) corresponding to forceps minor [Fig 2B(a)] and the splenium which includes the forceps major [Fig 2B(b)], both interhemispheric tracts. Two regions were selected from the frontal lobes. One labelled middle frontal white matter (FWM) [Fig 2B(c)], which encompasses the inferior frontal-occipital fasciculus, the anterior thalamic radiations and the lateral projections of the genu which run ipsilaterally. The other was a more inferolateral region of the FWM through which runs the superior longitudinal fasciculus [inferolateral FWM, Fig 2B(d)]. In the medial temporal lobe we selected the hippocampal part of the cingulum bundle [CGH, Fig 2B(e)]. White matter tracts, including cingulum, bilateral superior frontal-occipital fasciculus, and the genu of the CC are known to connect regions of the default mode network (Teipel *et al.*, 2010) which have been consistently found to be affected by Alzheimer's disease (Sorg *et al.*, 2009; Agosta *et al.*, 2011; Wu *et al.*, 2011). Furthermore, regions of the default mode network, such as the frontal lobes, are associated with working memory performance (Koshino *et al.*, 2014) whereas medial temporal lobe regions are involved in long-term associative memory functions (Ward *et al.*, 2014). These regions have shown a synergistic relationship following brain damage (Maccotta *et al.*, 2007). The final region of interest we considered was the centrum semiovale [Fig 2B(e)] which covers large areas of the corticospinal tract. This was chosen on the assumption of preserved motor functions in the early stages of Alzheimer's disease (Rose *et al.*, 2000; Huang *et al.*, 2012) and as such served as a comparative control region. One other region found to be relevant in previous DT-MRI studies involving preclinical Alzheimer's disease is the fornix (Ringman *et al.*, 2007; Molinuevo *et al.*, 2014; Racine *et al.*, 2014). This is a projection tract that connects the medial temporal lobe to other limbic structures and is known to be involved in memory functions (Boespflug *et al.*, 2014). However, technical limitations (i.e. small size and imprecise boundaries) prevented the inclusion of this region of interest in our analysis. Nevertheless, we included the CGH, a white matter tract linking the hippocampus and parahippocampal cortex to the posterior cingulate cortex, known to be relevant for memory function and sensitive to Alzheimer's disease pathology (Villain *et al.*, 2008; Catheline *et al.*, 2010).

Finally, region of interest selection was independently performed by two investigators of this study. The aim of this procedure was to assess inter-rater reliability of region of interest placement. To this aim, rater 2 (L.P.) randomly selected a subset of participants ($n = 5$) from the data set initially processed by rater 1 (H.S.). We report on the index of reproducibility and coefficient of variation for the two DT-MRI metrics.

Statistical analyses

Statistical analyses were performed in R version 3.1.1 (R Development Core Team). Group differences in background variables (e.g. age, education, and MMSE score) were examined with ANOVA using Tukey's test for *post hoc* comparisons. Hemispheric differences in fractional anisotropy and mean diffusivity values were examined with *t*-tests.

Group differences in behavioural tasks were tested with linear regression. A model with age, education, and group was created for each task (task ~ age + education + group) to test for the relationship between these variables and task performance. *Post hoc* group comparisons were performed with using pairwise least-squares means comparison with the Tukey's correction for multiple comparisons using lsmeans function from the lsmeans package. Least-squares means were used to extract the group means after controlling for age and education effects.

Group differences in DT-MRI metrics (i.e. fractional anisotropy and mean diffusivity values) for each region of interest were examined with linear regression. A simple model with group as a predictor was created for each region of interest (DT-MRI group) and *post hoc* group comparisons were performed with pairwise Tukey's test. This model, and the subsequent models in which 'Group' was entered as a predictor, allow the assessment of associations between dependent variables (i.e. DT-MRI measures and behavioural) and group membership. The rationale behind these regression models is that they fit the first intercept and slope for the association between such variables in the first group (in our analysis this was the healthy control group). Then, the models test whether group membership (i.e. asymptomatic carriers or patients with familial Alzheimer's disease) modifies such associations. The relationship between task performance and DT-MRI metrics was investigated with linear regression by fitting models with DT-MRI variables as predictors for task performance (task ~ DT-MRI).

Finally, the relationship between task performance, DT-MRI variables, and group membership was examined with correlation and linear regression. Firstly, we examined the correlation between task performance and DT-MRI variables in each region of interest separately in all groups. Second, to visualize the results, we examined the significant correlations revealed in step one more closely with linear regression. The relationship between task performance, group identity and DT-MRI parameters was investigated with linear regression by

predicting task performance with group identity, DT-MRI parameter, and their interaction ('task ~ group × DT-MRI'). To account for multiple statistical comparisons, all *P*-values shown were false detection rate (FDR) corrected.

A recent study confirmed that the method reported here to place regions of interest and derive DT-MRI variables provides good reliability (Pettit *et al.*, 2013). However, we performed further inter-rater reliability analysis for the regions of interest chosen for the present study. To this aim, placement of the regions of interest was independently performed by two investigators of this study. Rater 2 (L.P.) randomly selected a subset of participants ($n = 5$) from the data set initially processed by rater 1 (H.S.). We report on the index of reproducibility and coefficient of variation for the two DT-MRI variables.

Results

Behavioural results

Results from group comparisons of behavioural variables are presented in Table 2. Patients with familial Alzheimer's disease performed significantly worse than healthy controls on all neuropsychological and visual STM binding tasks except for the Wisconsin Card Sorting Test and Letter fluency task. Patients with familial Alzheimer's disease performed significantly worse than the asymptomatic carriers on all tasks except for the Copy of the Complex Rey Figure, the Trail Making Test part A, number of attempts to category in the Wisconsin Card Sorting Test, and the shape-colour binding task. Asymptomatic carriers performed significantly worse than healthy controls on the shape-colour binding condition of the visual STM task only.

Education was associated with task performance on the Trail Making Test, Animal Fluency, and Boston Naming Test. Age was not significantly associated with performance in any of the tasks. Importantly, age and education were not associated with visual STM shape-colour binding or PAL tasks, so further analyses with these tasks of interest did not include age or education as a covariate.

DT-MRI metrics

The inter-rater reliability analysis indicated excellent reproducibility of region of interest measurements with the standard deviation of the difference between repeated measures of mean diffusivity and fractional anisotropy being $37 \times 10^{-6}\,mm^2/s$ (mean of measurements $739 \times 10^{-6}\,mm^2/s$) and 0.034 (mean 0.349), respectively. This yielded coefficients of variation of 5.0% for mean diffusivity (range 0.0 for centrum semiovale to 8.51% for CGH) and 9.8% for fractional anisotropy (range 0.0 for centrum semiovale to 12.3% for CGH), which compares well with values for other studies using region of interest analysis (Shenkin *et al.*, 2005).

Initial comparisons between fractional anisotropy and mean diffusivity values from corresponding regions of interest in left and right hemispheres revealed hemispheric differences in all regions either in fractional anisotropy, mean diffusivity, or both. Therefore, all the reported analyses were conducted for hemispheres separately (Table 3). Group comparisons between asymptomatic carriers and

Table 2 Neuropsychological performance for the three groups

Model (task ~ age + education + group)		Predictor (beta and *P*-values)				*Post hoc* *t*-tests (*t* and *P*-values)		
Task	**R^2 (*P*-value)**	**Age**	**Education**	**Group 2 (AC)**	**Group 3 (FAD)**	**HC versus AC**	**HC versus FAD**	**AC versus FAD**
PAL	**0.47 (<0.001)**	−0.2 (0.108)	0.2 (0.130)	−0.2 (0.438)	**−9.6 (<0.001)**	0.8 (0.72)	**−4.4 (<0.001)**	**3.3 (0.005)**
Complex Rey Figure – copy	**0.30 (<0.001)**	−0.2 (0.221)	0.2 (0.159)	−0.02 (0.939)	**−7.0 (0.011)**	0.08 (0.997)	**2.7 (0.03)**	2.3 (0.06)
Complex Rey Figure – recall	**0.55 (<0.001)**	−0.01 (0.953)	0.2 (0.090)	0.07 (0.686)	**−1.19 (<0.001)**	−0.4 (0.913)	**5.6 (<0.001)**	**5.3 (<0.001)**
Letter fluency (FAS)	0.09 (0.068)	–	–	–	–	–	–	–
Animal fluency	**0.32 (<0.001)**	0.3 (0.059)	**0.3 (0.036)**	0.3 (0.209)	**−9.0 (0.001)**	−1.3 (0.417)	**3.5 (0.003)**	**4.1 (<0.001)**
Boston naming test	**0.35 (<0.001)**	0.2 (0.105)	**0.3 (0.04)**	0.2 (0.475)	**−10.0 (<0.001)**	−0.7 (0.753)	**3.9 (<0.001)**	**4.1 (<0.001)**
Word list – immediate recall	**0.45 (<0.001)**	<0.01 (1.000)	0.02 (0.847)	0.1 (0.493)	**−12.1 (<0.001)**	−0.7 (0.771)	**5.2 (<0.001)**	**5.2 (<0.001)**
Word list – delayed recall	**0.63 (<0.001)**	0.1 (0.449)	−0.01 (0.913)	−0.04 (0.830)	**−15.6 (<0.001)**	0.2 (0.975)	**8.2 (<0.001)**	**7.2 (<0.001)**
Word list recognition	**0.54 (<0.001)**	−0.1 (0.593)	−0.1 (0.423)	−0.01 (0.960)	**−13.5 (<0.001)**	0.05 (0.999)	**6.3 (<0.001)**	**5.6 (<0.001)**
Trail Making Test A	**0.38 (<0.001)**	0.3 (0.059)	**−0.2 (0.047)**	0.1 (0.827)	**6.39 (0.009)**	−0.2 (0.974)	**−2.7 (0.025)**	−2.1 (0.093)
WCST number of categories	**0.24 (0.002)**	0.1 (0.320)	0.2 (0.164)	**0.5 (0.030)**	**−6.3 (0.035)**	−2.2 (0.075)	2.2 (0.087)	**3.6 (0.002)**
WCST attempt to category	−0.07 (0.967)	–	–	–	–	–	–	–
Conditions of the VSTM Binding Task								
Shape only	**0.57 (<0.001)**	−0.2 (0.077)	0.04 (0.697)	−0.3 (0.062)	**−13.7 (<0.001)**	1.9 (0.147)	**6.4 (<0.001)**	**4.3 (<0.001)**
Colour only	**0.37 (<0.001)**	−0.1 (0.333)	0.07 (0.529)	−0.2 (0.281)	**−11.0 (<0.001)**	1.1 (0.525)	**4.3 (<0.001)**	**3.0 (0.01)**
Shape-colour binding	**0.42 (<0.001)**	−0.1 (0.458)	0.1 (0.242)	**−0.68 (0.001)**	**−12.6 (<0.001)**	**3.5 (0.003)**	**5.0 (<0.001)**	2.0 (0.133)

AC = asymptomatic carriers; FAD = familial Alzheimer's disease; HC = healthy controls; WCST = Wisconsin Card Sorting Test Significant. ($P < 0.05$) tests highlighted in bold. Beta values shown are standardized *P*-values for R^2 are FDR-corrected.

controls revealed no significant differences in either fractional anisotropy or mean diffusivity values. However, group comparisons between patients with familial Alzheimer's disease and controls showed that patients with familial Alzheimer's disease had higher mean diffusivity in CGH and genu CC bilaterally, left inferolateral FWM, and left splenium CC. Also, group comparisons between patients with familial Alzheimer's disease and asymptomatic carriers showed that patients with familial Alzheimer's disease had higher mean diffusivity in genu CC bilaterally, left inferolateral FWM, right CGH, and left splenium CC.

Relationship between DT-MRI metrics and behavioural tasks

To identify the regions of interest that might be related to deficits in STM binding, the shape-colour binding condition was chosen for further analysis as this was the only condition of the STM binding task that differentiated between the three study groups. Performance on the PAL task was also included for comparison due to the reported sensitivity of this memory function to the early stages of Alzheimer's disease (Swainson *et al.*, 2001; Fowler *et al.*, 2002). Although in the current study asymptomatic carriers were not significantly impaired on the PAL, in previous studies this task accounted for a large proportion of variance between carriers and controls who were taken from the same population (Parra *et al.*, 2010). Our data show a significant group effect in the shape-colour binding task (model $P < 0.001$, adjusted $R^2 = 0.42$) and PAL task (model $P < 0.001$, adjusted $R^2 = 0.43$).

In the shape-colour binding task, better performance was significantly predicted by mean diffusivity values in bilateral genu CC, left inferolateral FWM, and left CGH (Table 4). Fractional anisotropy values did not significantly predict task performance. When examining the groups separately, we found that task performance correlated significantly with mean diffusivity values in right middle FWM ($r = -0.80$, $P = 0.036$) and left genu CC ($r = -0.75$, $P = 0.04$) only in the familial Alzheimer's disease group (Fig. 3). In the other groups the correlations were not significant (Supplementary Table 3). The 'task ~ group × DT-MRI' model with variables showing significant correlations revealed that the slope of the familial Alzheimer's disease group significantly differed from that of controls for both middle FWM and bilateral genu CC (all $P < 0.05$).

In the PAL task, better performance was significantly predicted by fractional anisotropy values in left middle FWM, right splenium CC, left CGH, and by mean

Table 3 Significant group differences in DT-MRI measures in regions of interests

Model (DT-MRI ~ group)		Predictor (beta and *P*-values)		*Post-hoc* t-tests (t and *P*-values)		
DT-MRI	**R^2 (*P*-value)**	**Group 2 (AC)**	**Group 3 (FAD)**	**HC versus AC**	**HC versus FAD**	**AC versus FAD**
FA left mFWM	0.04 (0.224)	–	–	–	–	–
FA right mFWM	0.007 (0.417)	–	–	–	–	–
FA left iFWM	0.03 (0.224)	–	–	–	–	–
FA right iFWM	−0.005 (0.495)	–	–	–	–	–
FA left gCC	0.06 (0.133)	–	–	–	–	–
FA right gCC	−0.01 (0.568)	–	–	–	–	–
FA left sCC	−0.03 (0.850)	–	–	–	–	–
FA right sCC	−0.01 (0.527)	–	–	–	–	–
FA left CGH	0.10 (0.069)	–	–	–	–	–
FA right CGH	0.03 (0.224)	–	–	–	–	–
FA left CS	−0.003 (0.481)	–	–	–	–	–
FA right CS	0.06 (0.146)	–	–	–	–	–
⟨D⟩ left mFWM	0.07 (0.133)	–	–	–	–	–
⟨D⟩ right mFWM	0.08 (0.096)	–	–	–	–	–
⟨D⟩ left iFWM	**0.15 (0.024)**	0.04 (0.861)	**0.76 (0.003)**	−0.2 (0.983)	**−3.1 (0.008)**	**−2.9 (0.016)**
⟨D⟩ right iFWM	0.03 (0.234)	–	–	–	–	–
⟨D⟩ left gCC	**0.14 (0.024)**	0.07 (0.781)	**0.8 (0.003)**	−0.3 (0.958)	**−3.1 (0.008)**	**−2.8 (0.020)**
⟨D⟩ right gCC	**0.13 (0.036)**	−0.01 (0.969)	**0.70 (0.007)**	0.04 (0.999)	**−2.8 (0.018)**	**−2.8 (0.020)**
⟨D⟩ left sCC	**0.15 (0.024)**	−0.2 (0.409)	**0.63 (0.012)**	0.8 (0.685)	**−2.6 (0.032)**	**−3.3 (0.004)**
⟨D⟩ right sCC	0.005 (0.417)	–	–	–	–	–
⟨D⟩ left CGH	**0.16 (0.024)**	0.3 (0.287)	**0.85 (0.001)**	−1.1 (0.533)	**−3.5 (0.003)**	−2.4 (0.054)
⟨D⟩ right CGH	**0.24 (0.005)**	−0.1 (0.693)	**0.86 (<0.001)**	0.4 (0.917)	**−3.7 (0.001)**	**−4.0 (<0.001)**
⟨D⟩ left CS	0.11 (0.055)	–	–	–	–	–
⟨D⟩ right CS	0.005 (0.417)	–	–	–	–	–

⟨D⟩ = mean diffusivity; AC = asymptomatic carriers; CGH = hippocampal part of cingulum bundle; CS = centrum semiovale; FA = fractional anisotropy; FAD = familial Alzheimer's disease; gCC = genu of corpus callosum; HC = healthy controls; iFWM = inferior frontal white matter; mFWM = middle frontal white matter; sCC = splenium of corpus callosum. Significant ($P < 0.05$) tests highlighted in bold. *P*-values for R^2 are FDR-corrected.

diffusivity values in all regions of interest except the right inferolateral FWM and right centrum semiovale (Table 4). When examining the groups separately, we found that task performance correlated significantly with fractional anisotropy values in left middle FWM ($r = 0.85$, $P = 0.002$) and with mean diffusivity values in left middle FWM ($r = -0.69$, $P = 0.036$), right middle FWM ($r = -0.66$, $P = 0.048$), left inferolateral FWM ($r = 0.70$, $P = 0.036$), and left CGH ($r = -0.72$, $P = 0.036$) in the familial Alzheimer's disease group (Fig. 3). Although the correlations in the asymptomatic carriers group were all non-significant, the effect sizes were of middle or large magnitude as compared with small in the healthy control group (Supplementary Table 3). The 'task ~ group × DT-MRI' model with variables showing significant correlations revealed that the slope of the familial Alzheimer's disease group significantly differed from that of controls for fractional anisotropy values in left middle FWM, mean diffusivity in left middle FWM, left inferolateral FWM, and left CGH (all $P < 0.05$).

Discussion

The present study was designed to investigate whether white matter integrity detected with DT-MRI was associated with deficits in memory binding functions known to be sensitive to the early stages of Alzheimer's disease. This hypothesis was assessed in a unique population of carriers of the mutation E280A-PSEN1 who were either in the asymptomatic stages or had recently met criteria for Alzheimer's disease. The main findings of this study were: (i) white matter integrity in frontal regions (middle FWM) and in the anterior part of corpus callosum (genu CC) accounted for a significant proportion of variance of STM binding performance; (ii) white matter integrity in frontal regions (middle FWM and inferolateral FWM) and in the hippocampal part of cingulum bundle (CGH) accounted for a significant proportion of variance in performance on the PAL task; and (iii) these associations proved significant in the clinical but not in the preclinical stages of familial Alzheimer's disease. Before we discuss the implications of these findings for our current understanding of memory decline in Alzheimer's disease, we briefly address the distinction between these two memory systems.

STM binding is an integrative memory function known to support the conjunction of features necessary to create objects' identity (Staresina and Davachi, 2010). Such a function relies on regions along the visual ventral stream but is independent of the hippocampus (Parra *et al.*, 2014). Associative memory is an integrative memory function responsible for linking aspects of complex experiences, each with their own identity, into relational representations. Such a memory function cannot be carried out without an intact hippocampus (Moses and Ryan, 2006; Mayes *et al.*, 2007). Conjunctive (STM binding) and relational (associative memory) binding functions have been found to dissociate also in STM (Parra *et al.*, 2013). A recent hypothesis paper has suggested that context-free memory (e.g. STM binding) declines in the subhippocampal phase of Alzheimer's disease, which seems to occur very early in the disease process (Braak stages I–II). However, context-rich memory (e.g. associative memory) is impacted during the hippocampal phase of Alzheimer's disease which appears to correspond to more advanced diseases stages (Braak stages III–VI) (Didic *et al.*, 2011). This ongoing debate is relevant to our current study as our data revealed different patterns of dissociation for behavioural and DT-MRI variables.

Unlike previous studies which have consistently reported differences in white matter integrity in the presymptomatic stages of familial Alzheimer's disease (Ringman *et al.*, 2007; Ryan *et al.*, 2013), in the present study we failed to find significant differences in DT-MRI metrics between

Table 4 Variance explained by DT-MRI parameters in task performance in the STM binding task and the PAL task

Model (task ~ DT-MRI)	VSTM Shape-Colour Binding		PAL	
	FA R^2 (*P*-value), beta	⟨D⟩ R^2 (*P*-value), beta	FA R^2 (*P*-value), beta	⟨D⟩ R^2 (*P*-value), beta
Left mFWM	0.04 (0.157), 0.23	0.01 (0.276), −0.18	**0.18 (0.007), 0.44**	**0.14 (0.012), −0.40**
Right mFWM	0.05 (0.102), 0.27	0.02 (0.257), 0.19	0.02 (0.243), 0.20	**0.20 (0.007), −0.46**
Left iFWM	−0.02 (0.951), 0.009	**0.10 (0.040), −0.34**	0.00 (0.371), 0.15	**0.17 (0.007), −0.43**
Right iFWM	−0.00 (0.437), −0.13	0.08 (0.064), −0.31	0.01 (0.325), 0.16	0.06 (0.096), −0.27
Left gCC	−0.00 (0.414), 0.14	**0.15 (0.009), −0.41**	0.05 (0.115), 0.25	**0.22 (0.007), −0.48**
Right gCC	−0.01 (0.501), 0.11	**0.16 (0.009), −0.42**	−0.01 (0.501), 0.11	**0.17 (0.007), −0.43**
Left sCC	−0.02 (0.728), 0.06	0.03 (0.182), −0.22	0.06 (0.094), 0.27	**0.18 (0.024), −0.45**
Right sCC	−0.01 (0.501), 0.07	−0.02 (0.734), −0.06	**0.10 (0.032), 0.35**	**0.09 (0.040), −0.33**
Left CGH	−0.00 (0.414), 0.14	**0.15 (0.009), −0.41**	**0.13 (0.015), 0.39**	**0.20 (0.007), −0.46**
Right CGH	0.05 (0.112), 0.26	0.08 (0.066), −0.31	0.05 (0.107), 0.26	**0.18 (0.007), −0.44**
Left CS	−0.02 (0.782), −0.05	0.06 (0.094), −0.28	−0.02 (0.857), 0.03	**0.15 (0.009), −0.41**
Right CS	0.01 (0.325), 0.17	0.01 (0.299), −0.18	0.07 (0.071), 0.29	0.07 (0.007), −0.30

⟨D⟩ = mean diffusivity; CGH = hippocampal part of cingulum bundle; CS = centrum semiovale; FA = Fractional Anisotropy; gCC = genu of corpus callosum; iFWM = inferior frontal white matter; mFWM = middle frontal white matter; sCC = splenium of corpus callosum. Significant ($P < 0.05$) tests highlighted in **grey**. *P*-values are FDR-corrected.

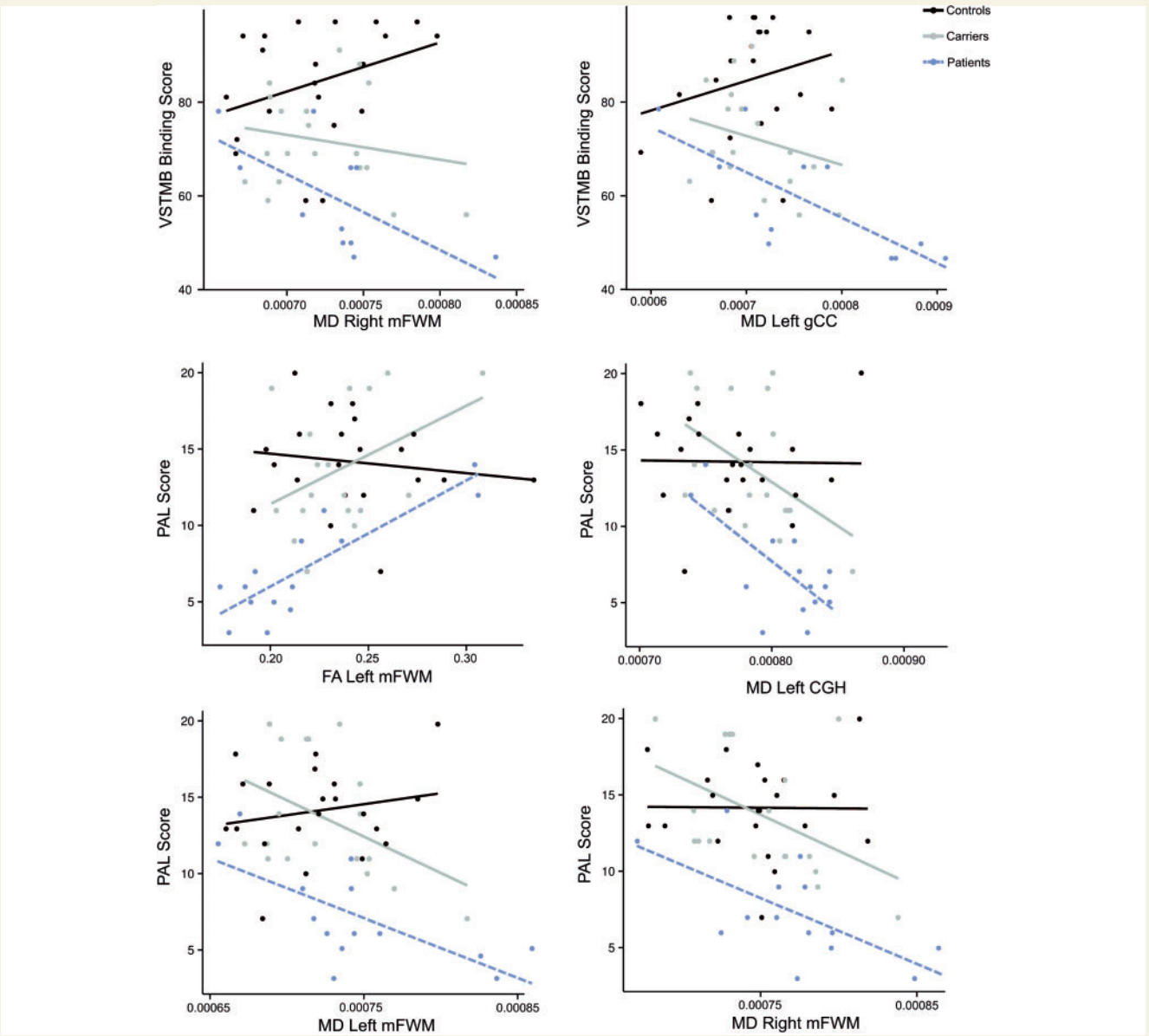

Figure 3 Regressions with region of interest, memory binding and group. Fitted regression lines for the shape-colour binding (*top*) and the PAL Task (*middle* and *bottom*) and DT-MRI variables for each group separately in the regions where significant correlations between DT-MRI metrics and memory performance were found. Dots show the observed data in raw values and lines represent fitted regression lines. CGH = hippocampal part of cingulum bundle; FA = fractional anisotropy; mFWM = middle FWM; MD = mean diffusivity; gCC = genu CC.

asymptomatic carriers and controls. There are some key differences between the present study and those reported earlier which may explain this lack of replication. First, Ringman *et al.* (2007) investigated DT-MRI metrics in a heterogeneous group of carriers of different mutations either in the *PSEN1* (A431E, $n = 11$; L235V, $n = 7$; G206A, $n = 1$) or *APP* gene (V717I, $n = 4$). This raises the question of whether such diverse genotypes may yield phenotypic expressions which contributed differently to the reported outcomes. In our study we assessed a sample taken from a population that carries a single mutation of PSEN1 (i.e. E280A). Second, the study by Ryan *et al.* (2013) investigated an even more genetically heterogeneous sample of carriers of PSEN1 mutation who were also older than the carriers investigated in the present study (mean age = 37.8 years, SD = 4.7). Age is an important factor in these dominantly inherited forms of Alzheimer's disease as it unequivocally indicates time to clinical expression. It has been recently observed that the PSEN1 mutation affecting the individuals from the Colombian kindred (i.e. E280A) leads to accumulation of amyloid deposits from 28 through to 37 years of age (Fleisher *et al.*, 2012). The asymptomatic carriers investigated here had a mean age of 35. The contributions of the amyloid pathology to white matter disruptions in Alzheimer's disease are well known (Racine *et al.*, 2014). These earlier findings together with our current results suggest that our sample of E280A-PSEN1 mutation carriers was in a stage of preclinical familial Alzheimer's

disease where structural damage to white matter tracts is not yet evident.

Consistent with previous studies (Parra *et al.*, 2010, 2011), mutation carriers who did and did not meet criteria for familial Alzheimer's disease presented with significant STM binding impairments. However, we observed that lower white matter integrity values were associated with STM binding impairments only in symptomatic carriers of the E280A-PSEN1 mutation. These differences were driven by increased mean diffusivity in frontal white matter and genu CC. One other study investigating white matter integrity in familial Alzheimer's disease of which we are aware (Ringman *et al.*, 2007), showed disruption in left frontal white matter (region of interest specified as two voxels in inferior FWM). Although Ringman *et al.* (2007) implemented a definition of frontal white matter different from our own, our results are complementary and suggest that FWM disturbance is an early anatomical signature of Alzheimer's disease (see also Oishi *et al.*, 2011*a*). Furthermore the present study indicates that these white matter differences are associated with a decline of memory functions known to be affected in the preclinical stages of the disease, namely STM binding.

The role of frontal lobes (and connecting structures such as genu CC) in working memory (Owen, 2000) and in binding functions in particular (Prabhakaran *et al.*, 2000; Sala and Courtney, 2007) has been recognized. Neuroimaging studies have documented the involvement of frontal regions, e.g. Brodmann area 10 and dorso-lateral prefrontal cortex, during feature binding in working memory (Prabhakaran *et al.*, 2000; Mitchell *et al.*, 2006) and have suggested that changes in the activity of these regions are related to reduced binding abilities in older adults (Mitchell *et al.*, 2006). Here this association is further strengthened with the finding of prefrontal tract abnormalities related to STM binding deficits in individuals who have recently met criteria for familial Alzheimer's disease. Neuronal degeneration in Alzheimer's disease seems to begin in the neuronal periphery rather than in the cell body (Pigino *et al.*, 2003; Stokin *et al.*, 2005), and these early abnormalities appear to be associated with amyloid pathology (Gunawardena and Goldstein, 2001; Racine *et al.*, 2014). Factors such as altered myelin and oligodendrocytes, axonal degeneration, and vascular pathologies, are some proposed mechanisms (Englund and Brun, 1990; Sjobeck *et al.*, 2005; Bartzokis *et al.*, 2007).

Severity of FWM damage in Alzheimer's disease is closely related to parenchymal Abeta load (Chalmers *et al.*, 2005). Recent studies in E280A-PSEN1 mutation carriers taken from the same population studied here show that amyloid-β deposits in frontal regions begin at the age of 27 years (range: 26.2–28.9) and reach a plateau at the age of 36.2 years (range: 35.1–39.3) (Fleisher *et al.*, 2012). This is more than 10 years before the average age of onset of this form of familial Alzheimer's disease. Of note, this is precisely the age at which we first see STM binding deficits in asymptomatic carriers of this mutation (Parra *et al.*, 2010, 2011), supporting the notion that these events, i.e. amyloid-β load, white matter degeneration and STM binding deficits, may be associated. However, contrary to our predictions, white matter integrity in the investigated region of interest did not correlate with STM binding performance in the preclinical stages of familial Alzheimer's disease. This raises the question of what disease mechanism could trigger such an early memory decline. A potential account could be offered by the Neuroplasticity Hypothesis of Alzheimer's disease (Teter and Ashford, 2002). Early amyloidosis in the course of Alzheimer's disease may disrupt synaptic transmission leading to neuronal connectivity impairments (Spires-Jones and Hyman, 2014). White matter synaptic disruption precedes both white matter tract anomalies and neurodegeneration (Alix and Domingues, 2011). Therefore, different memory binding functions may be affected by different white matter events which would range from early synaptic dysfunction (conjunctive binding functions) to large-scale network disruptions (relational binding functions). Such a hypothesis will benefit from future animal and human research.

Previous studies have reported that reduced white matter integrity in Alzheimer's disease leads to a disruption of the topological organization of large-scale structural networks (Lo *et al.*, 2010). We found that damage in middle FWM and genu CC were both related to poor performance on the STM binding task. The genu CC is a major white matter structure hosting tracts (e.g. forceps minor) which connect the dorsolateral prefrontal cortex across hemispheres (Barbas and Pandya, 1984). The strength of such connectivity seems to reflect changes in response to task demands (Tang *et al.*, 2010) or training (Takeuchi *et al.*, 2010). In the context of the present study, the association between poor performance on the binding condition of the STM task and increased mean diffusivity both in regional and trans-hemispheric white matter tracks may well reflect the demands for top-down attentional control. A recent functional MRI study which used the same STM binding task as the current investigation reported binding-specific activation in posterior parietal regions (Parra *et al.*, 2014) which are also known to be part of the network supporting top-down attentional control (Gazzaley and Nobre, 2012). Therefore, the hypothesis that STM binding deficits may be explained, at least in part, by impaired structural connectivity early in the course of familial Alzheimer's disease seems to be one supported by these data.

This study also sheds light on the neural substrate of PAL deficits in Alzheimer's disease and demonstrates that lower white matter integrity in frontal regions (middle FWM) and in the hippocampal part of cingulum bundle (CGH) accounts for a significant proportion of variance of performance on the PAL task in symptomatic carriers of the mutation. In line with previous studies, the patients with familial Alzheimer's disease assessed in the present study presented with associative learning deficits (Lowndes and Savage, 2007; Didic *et al.*, 2011). Associative memory, also known as relational binding (Moses and Ryan,

2006; Mayes *et al.*, 2007), seems to rely on the integrity of grey matter located in frontal regions and the hippocampus (Cer and O'Reilly, 2006) as well as on the effective connectivity between these regions (Fellgiebel and Yakushev, 2011; Yassa, 2011). There is evidence that associative learning declines in the prodromal stages of late-onset sporadic Alzheimer's disease (Swainson *et al.*, 2001; Fowler *et al.*, 2002). Previous neuroimaging studies in this population have demonstrated functional reorganization of medial temporal lobe structures, including the hippocampus, when asymptomatic carriers with an average age of 33.7 years completed a face-name association task (Quiroz *et al.*, 2010). The authors suggested that functional changes within the hippocampal memory system occur years before cognitive decline in familial Alzheimer's disease. In fact, Parra *et al.* (2010, 2011) showed that STM binding and PAL exhibit a gradual and continued decline in groups of carriers whose age approached the average age of onset of this familial Alzheimer's disease variant. This decline stood out from the neuropsychological background and was found to be earlier and much steeper in the former function. The results presented here suggest that these very early PAL impairments in the early stages of familial Alzheimer's disease are not solely due to the impact of neurodegeneration on grey matter structures (Quiroz *et al.*, 2013), but also to lower white matter integrity of those tracts connecting them.

It is worth noting that the analysis of DT-MRI metrics during PAL task performance revealed that this function relies on a more extended network than visual STM binding (Table 4). In previous studies we have found that STM binding was specifically affected by Alzheimer's disease relative to other non-Alzheimer's disease dementias (Della Sala *et al.*, 2012). We have suggested that a potential cause for this high specificity may lie at a neuroanatomical level. We have recently demonstrated that normal performance on the STM binding task presented here does not require an intact hippocampus (Parra *et al.*, 2013, 2014). In fact, we previously showed that performance on the STM binding and PAL tasks did not correlate in carriers of the mutations E280A-PSEN1 (Parra *et al.*, 2011). However, associative learning does decline in other non-Alzheimer's disease dementias (Taylor *et al.*, 1990; Dimitrov *et al.*, 1999; Clague *et al.*, 2005) and also in healthy ageing (Naveh-Benjamin *et al.*, 2007; Old and Naveh-Benjamin, 2008) rendering this task less specific both for the early detection of Alzheimer's disease and its differential diagnosis. In the present study we found that these functions previously dissociated at behavioural and anatomical level, also dissociate when the integrity of white matter structure is considered, reinforcing the notion that memory binding functions in STM and in LTM have different neural correlates. The fact that PAL relies on a widespread network whereas the STM binding relies on more restricted network may well explain the different pattern of sensitivity and specificity shown by these two memory binding functions.

A question that may arise from this study is whether the associations between lower white matter integrity and specific memory impairments reported here are typical of Alzheimer's disease or a phenotypic expression of this specific mutation (i.e. E280A-PSEN1). There is no straightforward answer to this question as the links between genotype and phenotype in Alzheimer's disease are poorly understood (Holmes, 2002). However, a recent study suggests that when it comes to STM binding, sporadic and familial variants of Alzheimer's disease share a common phenotype (Parra *et al.*, 2011). Moreover, the findings of DT-MRI studies of both sporadic and familial variants have been complementary suggesting that although triggered by different mechanisms, the clinical expression of white matter damage in these forms of Alzheimer's disease may also share phenotypic features (Gold *et al.*, 2012).

We acknowledge some limitations of this study. First, we used region of interest analyses which introduce some subjective components to the placement of region of interest structures of interest. However, we took great care in both the selection of regions of interest and their placement, while checks were performed to ensure they were placed solely in white matter structures. Furthermore, we assessed the inter-rater reliability as reported in a previous study (Pettit *et al.*, 2013) and this analysis confirmed a high reliability of this methods. We therefore consider it unlikely that issues related to the placement of regions of interest may have had an influence on the results reported here. Second, the lack of associations between memory binding performance and DT-MRI metrics in asymptomatic carriers may reflect limited power because of the relative small sample assessed in this study. This is supported by the finding of middle to large effect sizes for the correlational analyses between PAL performance and DTI-metrics in this group. Finally, it is worth mentioning some technical difficulties we encountered in identifying regions of interest such as the fornix, which is proving relevant as a biomarker for Alzheimer's disease (Oishi and Lyketsos, 2014). Although we failed to find significant associations between white matter integrity in the selected theory-driven region of interest and STM binding performance in the preclinical stages of familial Alzheimer's disease, there may still be white matter structures which are relevant to this cognitive function. Nevertheless, we have provided reliable evidence of dissociation between the integrity of white matter structures and the two memory functions investigated here, namely STM binding and associative learning.

In sum, the present study showed that reduced white matter integrity, in frontal lobes, corpus callosum and medial temporal lobes, can account for memory binding impairments in familial Alzheimer's disease. In the early stages of familial Alzheimer's disease, white matter integrity explained deficits in memory binding functions which rely on large-scale networks such as PAL. However, deficits in memory binding functions which need more selective networks do not seem to be accounted for by white matter

disruption in asymptomatic individuals who will unequivocally develop familial Alzheimer's disease. Future studies should investigate what particular disease mechanisms underpin such an early memory decline.

Funding

M.A.P. is supported by Alzheimer's Society, Grant # AS-R42303. The study is also sponsored by Colciencias, Grants 1115-408-20512 and 1115-343-19127 awarded to the Neuroscience Group, University of Antioquia, Colombia in collaboration with M.A.P. and S.D.S. The project was also partially supported by ALFA Eurocaribean Neurosciences Network, contract AML/B7-311/97/0666/II-0322-FA-FCD-FI-FC, in which S.D.S. and F.L. were partners. This work was conducted within the context of The University of Edinburgh Centre for Cognitive Ageing and Cognitive Epidemiology, part of the cross council Lifelong Health and Wellbeing Initiative (MR/K026992/1).

Supplementary material

Supplementary material is available at *Brain* online.

References

Agosta F, Pievani M, Geroldi C, Copetti M, Frisoni GB, Filippi M. Resting state fMRI in Alzheimer's disease: beyond the default mode network. Neurobiol Aging 2011; 33: 1564–78.

Alix JJ, Domingues AM. White matter synapses: form, function, and dysfunction. Neurology 2011; 76: 397–404.

Ardila A, Lopera F, Rosselli M, Moreno S, Madrigal L, Arango-Lasprilla JC, et al. Neuropsychological profile of a large kindred with familial Alzheimer's disease caused by the E280A single presenilin-1 mutation. Arch Clin Neuropsychol 2000; 15: 515–28.

Barbas H, Pandya DN. Topography of commissural fibers of the prefrontal cortex in the rhesus monkey. Exp Brain Res 1984; 55: 187–91.

Bartzokis G, Lu PH, Mintz J. Human brain myelination and amyloid beta deposition in Alzheimer's disease. Alzheimers Dement 2007; 3: 122–5.

Basser PJ. Inferring microstructural features and the physiological state of tissues from diffusion-weighted images. NMR Biomed 1995; 8: 333–44.

Berg EA. A simple objective test for measuring flexibility in thinking. J Gen Psychol 1948; 39: 15–22.

Boespflug EL, Eliassen J, Welge J, Krikorian R. Associative learning and regional white matter deficits in mild cognitive impairment. J Alzheimers Dis 2014; 41: 421–30.

Borroni B, Brambati SM, Agosti C, Gipponi S, Bellelli G, Gasparotti R, et al. Evidence of white matter changes on diffusion tensor imaging in frontotemporal dementia. Arch Neurol 2007; 64: 246–51.

Bozzali M, Cherubini A. Diffusion tensor MRI to investigate dementias: a brief review. Magn Reson Imaging 2007; 25: 969–77.

Bozzali M, Padovani A, Caltagirone C, Borroni B. Regional grey matter loss and brain disconnection across Alzheimer disease evolution. Curr Med Chem 2011; 18: 2452–8.

Buckner RL, Andrews-Hanna JR, Schacter DL. The brain's default network: anatomy, function, and relevance to disease. Ann N Y Acad Sci 2008; 1124: 1–38.

Buckner RL, Snyder AZ, Shannon BJ, LaRossa G, Sachs R, Fotenos AF, et al. Molecular, structural, and functional characterization of Alzheimer's disease: evidence for a relationship between default activity, amyloid, and memory. J Neurosci 2005; 25: 7709–17.

Buschke H, Kuslansky G, Katz M, Stewart WF, Sliwinski MJ, Eckholdt HM, et al. Screening for dementia with the memory impairment screen. Neurology 1999; 52: 231–8.

Catheline G, Periot O, Amirault M, Braun M, Dartigues JF, Auriacombe S, et al. Distinctive alterations of the cingulum bundle during aging and Alzheimer's disease. Neurobiol Aging 2010; 31: 1582–92.

Cer DM, O'Reilly RC. Neural mechanisms of binding in the hippocampus and neocortex: insights from computational models. In: Zimmer HD, Mecklinger A, Lindenberger U, editors. Handbook of binding and memory, perspective from cognitive neuroscience. New York: Oxford University Press; 2006. p. 193–220.

Chalmers K, Wilcock G, Love S. Contributors to white matter damage in the frontal lobe in Alzheimer's disease. Neuropathol Appl Neurobiol 2005; 31: 623–31.

Chua TC, Wen W, Slavin MJ, Sachdev PS. Diffusion tensor imaging in mild cognitive impairment and Alzheimer's disease: a review. Curr Opin Neurol 2008; 21: 83–92.

Clague F, Dudas RB, Thompson SA, Graham KS, Hodges JR. Multidimensional measures of person knowledge and spatial associative learning: can these be applied to the differentiation of Alzheimer's disease from frontotemporal and vascular dementia? Neuropsychologia 2005; 43: 1338–50.

Clark RF, Hutton M, Fuldner M, Froelich S, Karran E, Talbot C, et al. The structure of the presenilin 1 (S182) gene and identification of six novel mutations in early onset AD families. Nat Genet 1995; 11: 219–22.

Cook IA, Leuchter AF. Synaptic dysfunction in Alzheimer's disease: clinical assessment using quantitative EEG. Behav Brain Res 1996; 78: 15–23.

Della Sala S, Parra MA, Fabi K, Luzzi S, Abrahams S. Short-term memory binding is impaired in AD but not in non-AD dementias. Neuropsychologia 2012; 50: 833–40.

Didic M, Barbeau EJ, Felician O, Tramoni E, Guedj E, Poncet M, et al. Which memory system is impaired first in Alzheimer's disease? J Alzheimers Dis 2011; 27: 11–22.

Dimitrov M, Granetz J, Peterson M, Hollnagel C, Alexander G, Grafman J. Associative learning impairments in patients with frontal lobe damage. Brain Cogn 1999; 41: 213–30.

Douaud G, Jbabdi S, Behrens TE, Menke RA, Gass A, Monsch AU, et al. DTI measures in crossing-fibre areas: increased diffusion anisotropy reveals early white matter alteration in MCI and mild Alzheimer's disease. Neuroimage 2011; 55: 880–90.

Duan JH, Wang HQ, Xu J, Lin X, Chen SQ, Kang Z, et al. White matter damage of patients with Alzheimer's disease correlated with the decreased cognitive function. Surg Radiol Anat 2006; 28: 150–6.

Duchek JM, Cheney M, Ferraro FR, Storandt M. Paired associate learning in senile dementia of the Alzheimer type. Arch Neurol 1991; 48: 1038–40.

Dunkin JJ, Leuchter AF, Newton TF, Cook IA. Reduced EEG coherence in dementia: state or trait marker? Biol Psychiatry 1994; 35: 870–9.

Dvorine I. Quantitative classification of color blind. J Gen Psychol 1963; 68: 255–65.

Echavarri C, Aalten P, Uylings HB, Jacobs HI, Visser PJ, Gronenschild EH, et al. Atrophy in the parahippocampal gyrus as an early biomarker of Alzheimer's disease. Brain Struct Funct 2010; 215: 265–71.

Elias MF, Beiser A, Wolf PA, Au R, White RF, D'Agostino RB. The preclinical phase of alzheimer disease: A 22-year prospective study of the Framingham Cohort. Arch Neurol 2000; 57: 808–13.

Englund E, Brun A. White matter changes in dementia of Alzheimer's type: the difference in vulnerability between cell compartments. Histopathology 1990; 16: 433–9.

Fellgiebel A, Wille P, Muller MJ, Winterer G, Scheurich A, Vucurevic G, et al. Ultrastructural hippocampal and white matter alterations in mild cognitive impairment: a diffusion tensor imaging study. Dement Geriatr Cogn Disord 2004; 18: 101–8.

Fellgiebel A, Yakushev I. Diffusion tensor imaging of the hippocampus in MCI and early Alzheimer's disease. J Alzheimers Dis 2011; 26: 257–62.

Fleisher AS, Chen K, Quiroz YT, Jakimovich LJ, Gomez MG, Langois CM, et al. Florbetapir PET analysis of amyloid-beta deposition in the presenilin 1 E280A autosomal dominant Alzheimer's disease kindred: a cross-sectional study. Lancet Neurol 2012; 11: 1057–65.

Fowler KS, Saling MM, Conway EL, Semple JM, Louis WJ. Paired associate performance in the early detection of DAT. J Int Neuropsychol Soc 2002; 8: 58–71.

Gazzaley A, Nobre AC. Top-down modulation: bridging selective attention and working memory. Trends Cogn Sci 2012; 16: 129–35.

Gili T, Cercignani M, Serra L, Perri R, Giove F, Maraviglia B, et al. Regional brain atrophy and functional disconnection across Alzheimer's disease evolution. J Neurol Neurosurg Psychiatry 2011; 82: 58–66.

Gold BT, Johnson NF, Powell DK, Smith CD. White matter integrity and vulnerability to Alzheimer's disease: preliminary findings and future directions. Biochim Biophys Acta 2012; 1822: 416–22.

Gunawardena S, Goldstein LS. Disruption of axonal transport and neuronal viability by amyloid precursor protein mutations in Drosophila. Neuron 2001; 32: 389–401.

Holmes C. Genotype and phenotype in Alzheimer's disease. Br J Psychiatry 2002; 180: 131–4.

Huang H, Fan X, Weiner M, Martin-Cook K, Xiao G, Davis J, et al. Distinctive disruption patterns of white matter tracts in Alzheimer's disease with full diffusion tensor characterization. Neurobiol Aging 2012; 33: 2029–45.

Jenkinson M, Smith S. A global optimisation method for robust affine registration of brain images. Med Image Anal 2001; 5: 143–156.

Johnson DK, Barrow W, Anderson R, Harsha A, Honea R, Brooks WM, et al. Diagnostic utility of cerebral white matter integrity in early Alzheimer's disease. Int J Neurosci 2010; 120: 544–50.

Kantarci K, Petersen RC, Boeve BF, Knopman DS, Weigand SD, O'Brien PC, et al. DWI predicts future progression to Alzheimer disease in amnestic mild cognitive impairment. Neurology 2005; 64: 902–4.

Kaplan E, Gooidglass H, Weintraub S. Boston naming test. Philadelphia: Lea and Febiger; 1983.

Kiuchi K, Morikawa M, Taoka T, Nagashima T, Yamauchi T, Makinodan M, et al. Abnormalities of the uncinate fasciculus and posterior cingulate fasciculus in mild cognitive impairment and early Alzheimer's disease: a diffusion tensor tractography study. Brain Res 2009; 1287: 184–91.

Koenig T, Studer D, Hubl D, Melie L, Strik WK. Brain connectivity at different time-scales measured with EEG. Philos Trans R Soc Lond B Biol Sci 2005; 360: 1015–23.

Koshino H, Minamoto T, Yaoi K, Osaka M, Osaka N. Coactivation of the default mode network regions and working memory network regions during task preparation. Sci Rep 2014; 4: 5954.

Lo CY, Wang PN, Chou KH, Wang J, He Y, Lin CP. Diffusion tensor tractography reveals abnormal topological organization in structural cortical networks in Alzheimer's disease. J Neurosci 2010; 30: 16876–85.

Lopera F, Ardilla A, Martinez A, Madrigal L, rango-Viana JC, Lemere CA, et al. Clinical features of early-onset Alzheimer disease in a large kindred with an E280A presenilin-1 mutation. JAMA 1997; 277: 793–9.

Lowndes G, Savage G. Early detection of memory impairment in Alzheimer's disease: a neurocognitive perspective on assessment. Neuropsychol Rev 2007; 17: 193–202.

Maccotta L, Buckner RL, Gilliam FG, Ojemann JG. Changing frontal contributions to memory before and after medial temporal lobectomy. Cereb Cortex 2007; 17: 443–56.

Mayes A, Montaldi D, Migo E. Associative memory and the medial temporal lobes. Trends Cogn Sci 2007; 11: 126–35.

McKhann G, Drachman D, Folstein M, Katzman R, Price D, Stadlan EM. Clinical diagnosis of Alzheimer's disease: report of the NINCDS-ADRDA Work Group under the auspices of Department of Health and Human Services Task Force on Alzheimer's Disease. Neurology 1984; 34: 939–44.

Medina D, Detoledo-Morrell L, Urresta F, Gabrieli JD, Moseley M, Fleischman D, et al. White matter changes in mild cognitive impairment and AD: a diffusion tensor imaging study. Neurobiol Aging 2006; 27: 663–72.

Medina DA, Gaviria M. Diffusion tensor imaging investigations in Alzheimer's disease: the resurgence of white matter compromise in the cortical dysfunction of the aging brain. Neuropsychiatr Dis Treat 2008; 4: 737–42.

Miao X, Wu X, Li R, Chen K, Yao L. Altered connectivity pattern of hubs in default-mode network with Alzheimer's disease: an Granger causality modeling approach. PLoS One 2011; 6: e25546.

Mitchell KJ, Raye CL, Johnson MK, Greene EJ. An fMRI investigation of short-term source memory in young and older adults. Neuroimage 2006; 30: 627–33.

Molinuevo JL, Ripolles P, Simo M, Llado A, Olives J, Balasa M, et al. White matter changes in preclinical Alzheimer's disease: a magnetic resonance imaging-diffusion tensor imaging study on cognitively normal older people with positive amyloid beta protein 42 levels. Neurobiol Aging 2014; 35: 2671–80.

Morris JC, Heyman A, Mohs RC, Hughes JP, van BG, Fillenbaum G, et al. The Consortium to Establish a Registry for Alzheimer's Disease (CERAD). Part I. Clinical and neuropsychological assessment of Alzheimer's disease. Neurology 1989; 39: 1159–65.

Moses SN, Ryan JD. A comparison and evaluation of the predictions of relational and conjunctive accounts of hippocampal function. Hippocampus 2006; 16: 43–65.

Naveh-Benjamin M, Brav TK, Levy O. The associative memory deficit of older adults: the role of strategy utilization. Psychol Aging 2007; 22: 202–8.

O'Connell H, Coen R, Kidd N, Warsi M, Chin AV, Lawlor BA. Early detection of Alzheimer's disease (AD) using the CANTAB paired Associates Learning Test. Int J Geriatr Psychiatry 2004; 19: 1207–8.

O'Reilly RC, Busby RS, Soto R. Three forms of binding and their neural substrates: alternatives to temporal synchrony. In: Cleeremans A, editor. The unity of consciousness: binding, integration, and dissociation. Oxford: Oxford University Press; 2003. p. 168–92.

Oishi K, Mielke MM, Albert M, Lyketsos CG, Mori S. DTI analyses and clinical applications in Alzheimer's disease. J Alzheimers Dis 2011a; 26: 287–96.

Oishi K, Faria AV, Zijl P, Mori S. MRI atlas of human white matter. New York: Academic Press; 2011b.

Oishi K, Lyketsos CG. Alzheimer's disease and the fornix. Front Aging Neurosci 2014; 6: 241.

Old SR, Naveh-Benjamin M. Differential effects of age on item and associative measures of memory: a meta-analysis. Psychol Aging 2008; 23: 104–18.

Osterrieth PA. Le test de copie d'une figure complex: contribution a l'etude de la perception et de la memoire. Arch Psychol 1944; 30: 206–356.

Owen AM. The role of the lateral frontal cortex in mnemonic processing: the contribution of functional neuroimaging. [Review]. Exp Brain Res 2000; 133: 33–43.

Parra MA, Della Sala S, Logie RH, Morcom AM. Neural correlates of shape-color binding in visual working memory. Neuropsychologia 2014; 52: 27–36.

Parra MA, Fabi K, Luzzi S, Cubelli R, Hernandez VM, Della Sala S. Relational and conjunctive binding functions dissociate in short-term memory. Neurocase 2013; 21: 56–66.

Parra MA, Abrahams S, Fabi K, Logie R, Luzzi S, Della Sala S. Short-term memory binding deficits in Alzheimer's disease. Brain 2009; 132: 1057–66.

Parra MA, Abrahams S, Logie RH, Mendez LG, Lopera F, Della Sala S. Visual short-term memory binding deficits in familial Alzheimer's disease. Brain 2010; 133: 2702–13.

Parra MA, Sala SD, Abrahams S, Logie RH, Mendez LG, Lopera F. Specific deficit of colour-colour short-term memory binding in sporadic and familial Alzheimer's disease. Neuropsychologia 2011; 49: 1943–52.

Pettit LD, Bastin ME, Smith C, Bak TH, Gillingwater TH, Abrahams S. Executive deficits, not processing speed relates to abnormalities in distinct prefrontal tracts in amyotrophic lateral sclerosis. Brain 2013; 136: 3290–304.

Pigino G, Morfini G, Pelsman A, Mattson MP, Brady ST, Busciglio J. Alzheimer's presenilin 1 mutations impair kinesin-based axonal transport. J Neurosci 2003; 23: 4499–508.

Pihlajamaki M, Sperling RA. Functional MRI assessment of task-induced deactivation of the default mode network in Alzheimer's disease and at-risk older individuals. Behav Neurol 2009; 21: 77–91.

Prabhakaran V, Narayanan K, Zhao Z, Gabrieli JD. Integration of diverse information in working memory within the frontal lobe. Nat Neurosci 2000; 3: 85–90.

Quiroz YT, Stern CE, Reiman EM, Brickhouse M, Ruiz A, Sperling RA, et al. Cortical atrophy in presymptomatic Alzheimer's disease presenilin 1 mutation carriers. J Neurol Neurosurg Psychiatry 2013; 84: 556–61.

Quiroz YT, Budson AE, Celone K, Ruiz A, Newmark R, Castrillón G, et al. Hippocampal hyperactivation in presymptomatic familial Alzheimer's disease. Ann Neurol 2010; 68: 865–75.

Racine AM, Adluru N, Alexander AL, Christian BT, Okonkwo OC, Oh J, et al. Associations between white matter microstructure and amyloid burden in preclinical Alzheimer's disease: a multimodal imaging investigation. Neuroimage Clin 2014; 4: 604–14.

Reitan RM. Validity of the Trail Making test as an indicator of organic brain damage. Percept Motor Skills 1958; 8: 271–6.

Ringman JM, O'Neill J, Geschwind D, Medina L, Apostolova LG, Rodriguez Y, et al. Diffusion tensor imaging in preclinical and presymptomatic carriers of familial Alzheimer's disease mutations. Brain 2007; 130: 1767–76.

Rose SE, Chen F, Chalk JB, Zelaya FO, Strugnell WE, Benson M, et al. Loss of connectivity in Alzheimer's disease: an evaluation of white matter tract integrity with colour coded MR diffusion tensor imaging. J Neurol Neurosurg Psychiatry 2000; 69: 528–30.

Ryan NS, Keihaninejad S, Shakespeare TJ, Lehmann M, Crutch SJ, Malone IB, et al. Magnetic resonance imaging evidence for presymptomatic change in thalamus and caudate in familial Alzheimer's disease. Brain 2013; 136: 1399–414.

Sala JB, Courtney SM. Binding of what and where during working memory maintenance. Cortex 2007; 43: 5–21.

Sexton CE, Kalu UG, Filippini N, Mackay CE, Ebmeier KP. A meta-analysis of diffusion tensor imaging in mild cognitive impairment and Alzheimer's disease. Neurobiol Aging 2011; 32: 2322.

Shenkin SD, Bastin ME, Macgillivray TJ, Deary IJ, Starr JM, Rivers CS, et al. Cognitive correlates of cerebral white matter lesions and water diffusion tensor parameters in community-dwelling older people. Cerebrovasc Dis 2005; 20: 310–18.

Sjobeck M, Haglund M, Englund E. Decreasing myelin density reflected increasing white matter pathology in Alzheimer's disease—a neuropathological study. Int J Geriatr Psychiatry 2005; 20: 919–26.

Sorg C, Riedl V, Perneczky R, Kurz A, Wohlschlager AM. Impact of Alzheimer's disease on the functional connectivity of spontaneous brain activity. Curr Alzheimer Res 2009; 6: 541–53.

Spires-Jones TL, Hyman BT. The intersection of amyloid beta and tau at synapses in Alzheimer's disease. Neuron 2014; 82: 756–71.

Staresina BP, Davachi L. Object unitization and associative memory formation are supported by distinct brain regions. J Neurosci 2010; 30: 9890–7.

Stebbins GT, Murphy CM. Diffusion tensor imaging in Alzheimer's disease and mild cognitive impairment. Behav Neurol 2009; 21: 39–49.

Stokin GB, Lillo C, Falzone TL, Brusch RG, Rockenstein E, Mount SL, et al. Axonopathy and transport deficits early in the pathogenesis of Alzheimer's disease. Science 2005; 307: 1282–8.

Sumerall SW, Timmons PL, James AL, Ewing MJ, Oehlert ME. Expanded norms for the Controlled Oral Word Association Test. J Clin Psychol 1997; 53: 517–21.

Swainson R, Hodges JR, Galton CJ, Semple J, Michael A, Dunn BD, et al. Early detection and differential diagnosis of Alzheimer's disease and depression with neuropsychological tasks. Dement Geriatr Cogn Disord 2001; 12: 265–80.

Sweed HS, Abdul-Rahman SA, Abdel-Aal WM, Abdul-Rahman LA. Clock drawing testing and diffusion tensor imaging among vascular dementia versus Alzheimer's disease. European Geriatric Medicine 2012; 3: 349–55.

Takeuchi H, Sekiguchi A, Taki Y, Yokoyama S, Yomogida Y, Komuro N, et al. Training of working memory impacts structural connectivity. J Neurosci 2010; 30: 3297–303.

Tang CY, Eaves EL, Ng JC, Carpenter DM, Mai X, Schroeder DH, et al. Brain networks for working memory and factors of intelligence assessed in males and females with fMRI and DTI. Intelligence 2010; 38: 293–303.

Taylor AE, Saint-Cyr JA, Lang AE. Memory and learning in early Parkinson's disease: evidence for a "frontal lobe syndrome". Brain Cogn 1990; 13: 211–32.

Teipel SJ, Bokde AL, Meindl T, Amaro E Jr, Soldner J, Reiser MF, et al. White matter microstructure underlying default mode network connectivity in the human brain. Neuroimage 2010; 49: 2021–32.

Teter B, Ashford JW. Neuroplasticity in Alzheimer's disease. J Neurosci Res 2002; 70: 402–37.

Ukmar M, Makuc E, Onor ML, Garbin G, Trevisiol M, Cova MA. Evaluation of white matter damage in patients with Alzheimer's disease and in patients with mild cognitive impairment by using diffusion tensor imaging. Radiol Med 2008; 113: 915–22.

Villain N, Desgranges B, Viader F, De lS V, Mezenge F, Landeau B, et al. Relationships between hippocampal atrophy, white matter disruption, and gray matter hypometabolism in Alzheimer's disease. J Neurosci 2008; 28: 6174–81.

Wang J, Zuo X, Dai Z, Xia M, Zhao Z, Zhao X, et al. Disrupted Functional Brain Connectome in Individuals at Risk for Alzheimer's Disease. Biol Psychiatry 2012; 73: 472–81.

Ward AM, Schultz AP, Huijbers W, van Dijk KR, Hedden T, Sperling RA. The parahippocampal gyrus links the default-mode cortical network with the medial temporal lobe memory system. Hum Brain Mapp 2014; 35: 1061–73.

Wechsler D. The Wechsler memory scale-III UK manual. San Antonio, TX: Psychological Corporation; 1997.

Wu X, Li R, Fleisher AS, Reiman EM, Guan X, Zhang Y, et al. Altered default mode network connectivity in Alzheimer's disease–a resting functional MRI and Bayesian network study. Hum Brain Mapp 2011; 32: 1868–81.

Yassa MA. Searching for novel biomarkers using high resolution diffusion tensor imaging. J Alzheimers Dis 2011; 26 3: 297–305.

Zhuang L, Wen W, Zhu W, Trollor J, Kochan N, Crawford J, et al. White matter integrity in mild cognitive impairment: a tract-based spatial statistics study. Neuroimage 2010; 53: 16–25.